Royal Norwegian Council
for Scientific and Industrial Research
(NTNF)

NORSAR

NORSAR Scientific Report No. 2-87/88

Semiannual Technical Summary

1 October 1987 – 31 March 1988

L.B. Loughran (ed.)

Kjeller, June 1988

VII.4 Coupling of short period surface wavetrains across the North Sea Graben

In the previous semiannual technical report (Maupin, 1987), we briefly presented a coupling method aiming at modelling surface wave propagation in 2-D structures, and some preliminary results. The method is now applied to a model of the North Sea Graben. We examine how a large-scale and very strong lateral variation of the crustal structure affects the propagation of the short-period surface wave trains.

Model

We use a simplified 2-D model of the North Sea Graben devised by Kennett and Mykkeltveit (1984), based on seismic refraction profiling experiments reported by Wood and Barton (1983). The model consists of purely elastic homogeneous layers of laterally varying thicknesses (Fig. VII.4.1). It is extended at depth with a 60 km thick lid, having S-wave velocities increasing from 4.65 to 4.71 km/s. The Rg, Lg and Sn wavetrains that we aim to study are supported by these crustal and lid waveguides. Due to the lateral variation of the waveguides, the wavetrains may radiate body waves, which leave the structure to propagate deeper in the mantle. The body waves can be represented by a sum of surface wave modes, as required by the coupling method, by extending the model to depths where the S-velocity is as large as the largest horizontal apparent velocity of the radiated body waves. The mantle underneath the North Sea presents a low-velocity zone (Stuart, 1978). In such a structure, a large number of modes propagate, many of them having very little energy in crustal and lid waveguides. Thus using a realistic model of the mantle requires to use a large number of modes to model the body wavefield propagating in the crust and in the lid, most of the modes having a very small contribution to the wavefield. A least-cost approximation is available with the locked mode method (Harvey, 1981); the introduction of a half-space with a very high S-wave velocity underneath the structure of interest creates trapped modes with high phase velocities able to represent the body

waves with a minimum number of modes. We thus introduce a halfspace with an S-wave velocity of 7.0 km/s underneath the lid to complete the model.

The model is divided into 51 zones, 25 equally wide zones in each laterally heterogeneous outer part of the Graben, and one 50 km wide zone in the central part of the Graben. The 26 first Rayleigh wave modes and the 26 first Love wave modes are calculated in each zone at a period of 1.0 s using the subroutine package of Saito (1988). The vertical displacement with depth of the Rayleigh wave local modes at the outskirts of the Graben are plotted on Fig. VII.4.2, where they are classified according to the wavetrain they belong to. The necessity to retain only a reasonable amount of modes leads us to neglect body waves with higher apparent phase velocities than 5.1 km/s. The phase velocities of the different modes are plotted as a function of horizontal distance in the Graben on Fig. VII.4.3 for Rayleigh wave modes and on Fig. VII.4.4 for Love wave modes. The zonal phase velocities are superimposed on the local phase velocities, issued as a subproduct of the coupling method. We can notice the good agreement between the velocities calculated with the two methods. The very fine zoning in the laterally varying parts of the model is required by the non-linearity of the sedimentary layer influence, specially on the Rayleigh wave modes, testified by the oscillatory behavior of the phase velocities with distance on Fig. VII.4.3.

Transmission properties

Through propagation across the Graben, the different modes are coupled by the lateral heterogeneity. Due to the large scale of the model compared to the wavelengths of the modes involved in this study, the coupling in reflection is very small. For Rayleigh waves propagating perpendicularly to the Graben for example, only 0.02% of the incoming energy is reflected by the structure. We will therefore concentrate our attention on the transmission properties of the structure.

We study the transmission properties for 2 different wave propagation directions. First for waves propagating in the x-direction of the structure lateral variation. And second for waves propagating at an angle with respect to this direction. Since coupling occurs between modes having a common slowness in the y-direction parallel to the Graben structure, and that the modes involved in the coupling have different total slownesses, they all propagate in slightly different directions in the second case. As an example, we have chosen to treat the case of a slowness in the y-direction equal to 1 s/km. This corresponds to propagation with respect to the x-direction at 22° for the Rg-wavetrain, 25 to 45° for the Lg-wavetrain, around 48° for the Sn wave, and from 49 to 58° for the body waves.

The transmission matrices express how the energy of an incoming mode is distributed on the different modes of the system after propagation across the Graben. The matrix elements on Figs. VII.4.5 to VII.4.8 are the absolute values of the amplitude transmission coefficients expressed in %, for modes normalized to a unit energy flux. The square elements thus represent energy transmission coefficients. Each column of the matrix corresponds to a different incoming wave.

For propagation at right angle across the Graben, the Rayleigh and Love wave modes are decoupled. On Fig. VII.4.5 is plotted the transmission matrix for the Rayleigh wave modes, and on Fig. VII.4.6 for the Love wave modes. In this model, the fundamental mode of the Rayleigh waves, or the Rg wavetrain, is little affected by the lateral heterogeneity. It has hardly any coupling with adjacent modes (Fig. VII.4.5). We should notice that this results from the homogeneous velocities of the sedimentary layer of this model, where the Rayleigh wave fundamental mode at 1 Hz is confined. With a refined representation of the sediments, the Rg wavetrain might be more affected by the Graben structure. Among the other Rayleigh wave modes of Fig. VII.4.5, the Lg modes are strongly coupled to each other as well as to the Sn modes. Their coupling is weaker with the body wave modes. The Sn modes are

strongly coupled both to the Lg modes and to the body waves. And symmetrically, the SV body waves are strongly coupled to the Sn modes, but weakly to the Lg ones. The partition of the modal set into different wavetrains associated with different waveguides is clearly mirrored by the transmission matrix. The strongest couplings appear to be restricted to neighboring waveguides. The coupling pattern is somewhat more complex for the Love wave modes (Fig. VII.4.6). For the Love waves, the coupling of the Lg wave modes is fairly strong both with the Sn wave and the body waves, and the Sn wave modes are strongly coupled with Lg as well as with body wave modes.

Figs. VII.4.7 and VII.4.8 display the transmission matrices for Rayleigh and Love waves propagating at an angle with respect to the x-direction. The shift of the propagation direction away from the direction of lateral variation of the structure does not strongly alter the coupling among the Rayleigh wave modes or among the Love wave modes. The new feature is the coupling between the Love and Rayleigh wave modes, which remains nonetheless very small.

In order to summarize the results quantitatively, we transform the transmission matrices, expressed as mode to mode coupling coefficients, into energy transfers from wavetrain to wavetrain. Since the coupling between two wavetrains depends on the modal content, both in amplitude and in phase, of the incoming wavetrain, we average out over amplitudes and phases in order to obtain a mean coupling, comparable to a general trend in a set of seismograms. Averaging out the amplitudes is equivalent to using a wavetrain where the energy is equally distributed among the different modes. The energy carried by a mode or a wavetrain is also distributed with depth differently from one mode to another, and therefore does not directly predict the amplitude of its surface displacement. The energy transfers need thus also to be converted into wavetrain amplitudes at the surface of the model to be directly comparable to observed seismograms.

In Table VII.4.1, we give the percentage of energy distributed on the different wavetrains of the system (1st column) after propagation across the Graben, for different incoming wavetrains. The energy distribution is also transcribed into surface amplitudes (2nd column) scaled to the surface amplitude of the incoming wavetrain. We use the vertical displacement for the Rayleigh waves. The two first parts of the table deal with Rayleigh and Love waves propagating at right angle across the Graben. The lower part of the table displays the coupling among wavetrains propagating across the North Sea Graben in a direction non-perpendicular to the symmetry direction of the structure. The most significant features of the table are expressed as diagrams on Figs. VII.4.9 to VII.4.11.

The properties of the transmission matrices are of course mirrored into the parts of the table and diagrams related to energy transmission. We recognize the independence of Rg wavetrain (Fig. VII.4.9a). Whether they are of Rayleigh or Love type, and whether they propagate in a direction perpendicular or not to the structure, the Lg wavetrains leak only a small fraction of their energy in the Sn wave and in the body waves (Fig. VII.4.9b, 9c and 10). The energy transferred from Rayleigh to Love wave modes (Fig. VII.4.9c) or conversely (Fig. VII.4.10b) when the propagation direction is at an angle with respect to the structure, is very small. Fig. VII.4.11 displays the strong transfer from Sn to Lg and body-wave energy.

If we now turn to the transcription of these energy transfers into surface displacement amplitudes, we notice that the transfers from Lg to Sn waves, which shift some energy depthward, reduce the total amplitude of the signal (see Fig. VII.4.9b and 10a, where the amplitude of the body waves, transferred into deeper parts of the earth, should not be considered as part of the signal). On the other hand, the strong conversion from Sn to Lg produces an Lg surface signal at the exit of the Graben 2.5 times larger than the original surface displace-

ment for Rayleigh waves (Fig. VII.4.11) and 3 times larger for Love waves.

Similarly, and despite the small amount of energy involved, transfers from Rayleigh to Love modes enhance the surface displacement significantly. For example, we observe on Fig. VII.4.9c that the total Lg wavetrain at the exit of the Graben presents a transversal displacement (associated with Love wave modes) up to 0.3 times the vertical displacement (associated with Rayleigh wave modes). Conversely, transfers from Love to Rayleigh wave modes does not produce such a significant vertical surface displacement (Fig. VII.4.10b). This results from the general property of the surface displacements around 1 Hz, which are on the average twice as large for Lg Love wave modes as for Lg Rayleigh wave modes, for a similar amount of energy at depth. This property predicts that, if after some strong couplings, the energy becomes equally distributed among Love and Rayleigh modes, the transversal component of the Lg wavetrain is twice as large as the vertical one.

Conclusion

We find a mean energy transmission across the North Sea Graben of 80% for an Lg wavetrain at 1 Hz. This is in apparent contradiction with the extinction of the Lg phase across this structure, as observed by Kennett and Mykkeltveit (1984). Even if we include more modes in order to better account for the body waves propagating in the mantle, and thereby decrease the amount of energy confined in the waveguides, it seems unlikely that this will prove sufficient to reconcile modelling results and observations. These results deal only with the amplitude of the transmission matrix at a given period. The phase behavior of the wave as a function of period is a key-element to the effective build-up of a wavetrain. Further tests need thus to be performed to study how the phase of the transmission matrix varies with period. If rapid variations are observed, destructive interferences between neighboring periods might explain the disappearance of the Lg wavetrain. Further-

more, our modelling accounts only for the gross features of the Graben. Other phenomena, such as a strong attenuation or particularly important small-scale heterogeneities able to reflect energy, might be associated with the sedimentary thickening and the Moho uprising to explain the extinction of the Lg phase.

On the other hand, our results concerning Rayleigh-Love couplings are in better agreement with observations of anomalously high transversal motions on Lg wavetrains (Kennett and Mykkeltveit, 1984) for explosive sources. Despite a level of coupling rather low in the above example, we show how the couplings from Rayleigh to Love waves enhance the total displacement, whereas couplings from Love to Rayleigh waves lower it, and that strong couplings produce Lg transversal surface displacement twice as large as the vertical one.

V. Maupin, Postdoctorate
Fellow

References

Harvey, D.J. (1981): Seismogram synthesis using normal mode superposition: the locked mode approximation. Geophys. J.R. astr. Soc., 66, 37-70.

Kennett, B.L.N. and S. Mykkeltveit (1984): Guided wave propagation in laterally varying media. II: Lg waves in northwestern Europe. Geophys. J.R. astr. Soc., 79, 257-267.

Maupin, V. (1987): Preliminary tests for surface waves in 2-D structures. Semiann. Tech. Summary, 1 Apr - 30 Sep 1987, NORSAR Sci. Rep. No. 1-87/88, Kjeller, Norway.

Saito, M. (1988): Disper80: a subroutine package for the calculation of seismic normal mode solutions. In: D.J. Doornbos (ed.), Seismological Algorithms, Academic Press.

Stuart, G.W. (1978): The upper mantle structure of the North Sea region from Rayleigh wave dispersion. Geophys. J.R. astr. Soc., 52, 367-382.

Wood, R. and P. Barton (1983): Crustal thinning and subsidence in the North Sea. Nature, 302, 134-136.

Propagation perpendicular to the Graben

Rayleigh waves

Input / Output	Rg		Lg		Sn	
Rg	99.667	0.9983	0.026	0.0297	0.002	0.0826
Lg	0.281	0.0278	79.172	0.8837	37.043	2.4583
Sn	0.007	0.0004	10.071	0.0347	18.139	0.2903
P/Sv	0.038	0.0012	10.735	0.0436	44.810	0.8721

Love waves

Input / Output			Lg		Sn	
Lg			78.560	0.9038	22.100	3.0854
Sn			3.692	0.0242	48.885	0.6393
Sh			17.751	0.1899	29.021	1.7655

Propagation at an angle with the Graben

Input / Output	R Rg		R Lg		R Sn	
R Rg	99.737	0.9987	0.015	0.0229	0.001	0.0402
R Lg	0.168	0.0206	76.146	0.8628	33.267	4.9471
R Sn	0.002	0.0002	9.083	0.0327	11.992	0.3345
R P/Sv	0.027	0.0008	12.774	0.0489	53.874	0.8546
L Lg	0.048	0.0295	1.325	0.2538	0.601	1.1842
L Sn	0.004	0.0010	0.207	0.0128	0.065	0.0655
L Sh	0.012	0.0054	0.446	0.0616	0.193	0.3828
Input / Output			L Lg		L Sn	
R Rg			0.004	0.0052	0.002	0.0302
R Lg			1.214	0.0477	1.143	0.3451
R Sn			0.151	0.0019	0.098	0.0122
R P/Sv			0.688	0.0045	0.284	0.0222
L Lg			77.177	0.8926	26.910	3.5245
L Sn			4.459	0.0266	42.850	0.6438
L Sh			16.311	0.1756	28.719	1.6148

Table VII.4.1 Wavetrain coupling at 1 Hz by propagation across the North Sea Graben. The left columns give the energy distribution in %, and the right columns give the surface displacement amplitudes, normalized to the surface displacement of the incoming wave, of the different wavetrains, at the exit of the model. Rayleigh wavetrains are noted R and Love wavetrains are noted L.

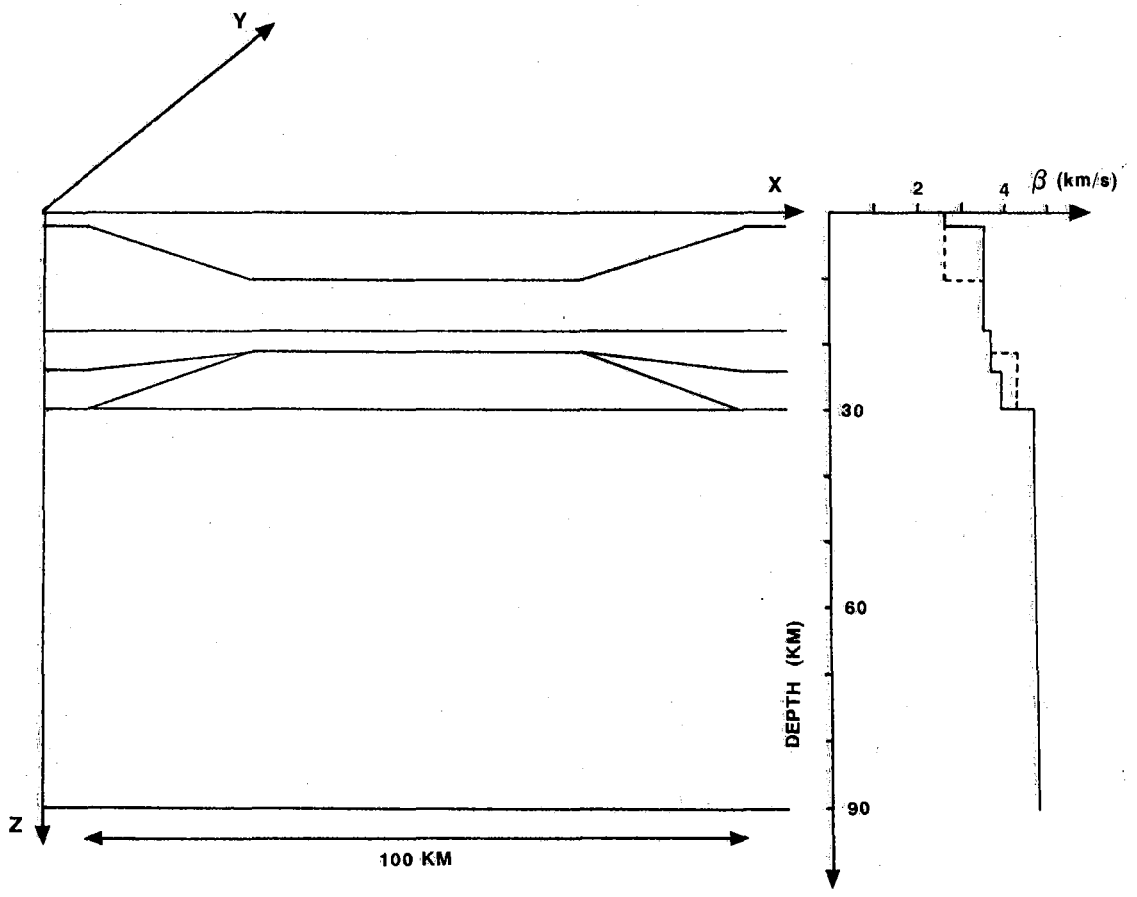

Fig. VII.4.1 Model of the North Sea Graben (after Kennett and Mykkeltveit, 1984).

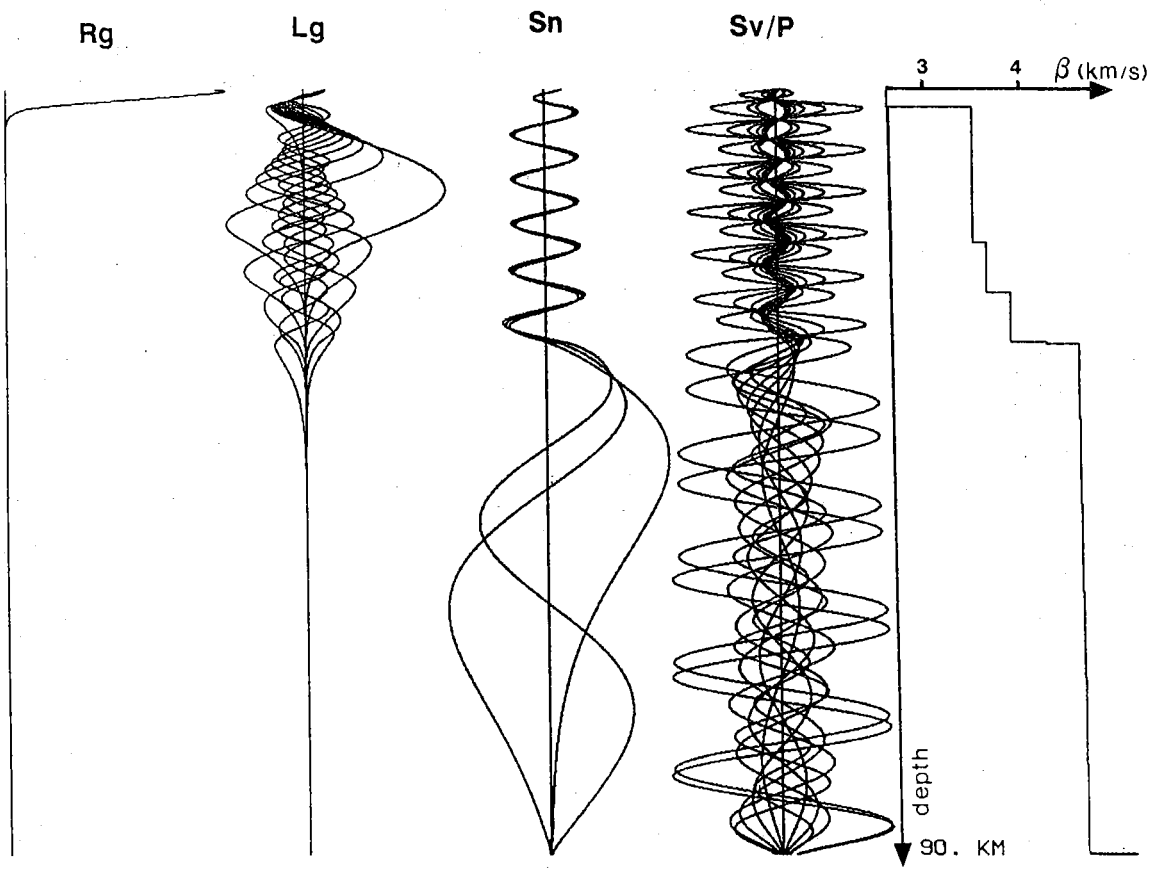

Fig. VII.4.2 Vertical displacement as a function of depth of the 26 first Rayleigh wave modes at 1 Hz at the outskirts of the North Sea Graben. The modes are classified according to the wavetrain they belong to. The S-wave velocity as a function of depth is plotted for reference.

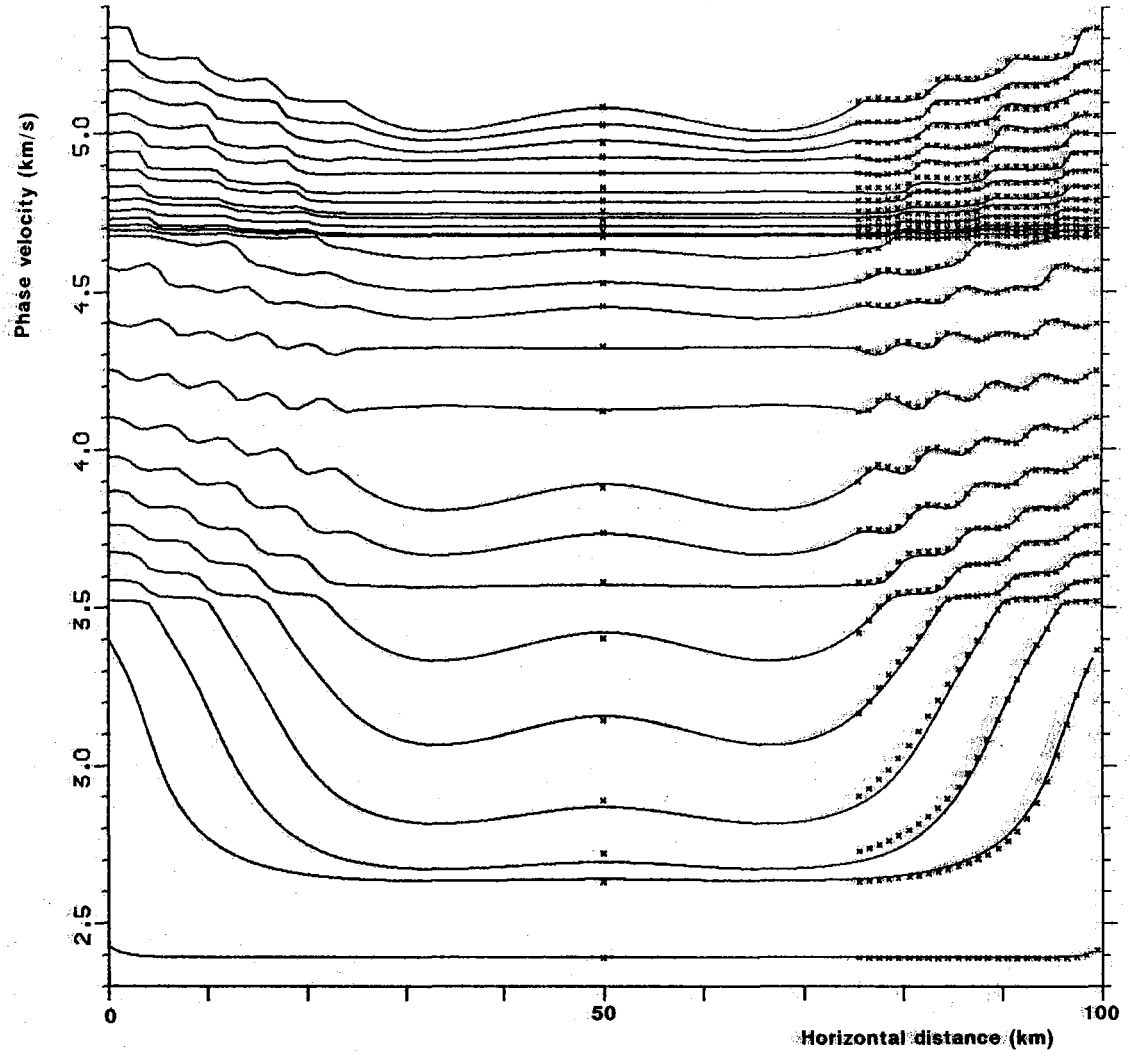

Fig. VII.4.3 Phase velocities of the 26 first Rayleigh wave modes as a function of horizontal distance in the North Sea Graben model, at 1 Hz. The lines represent the phase velocities integrated by the coupling method, and the crosses represent the zonal phase velocities (with omission of the left side crosses).

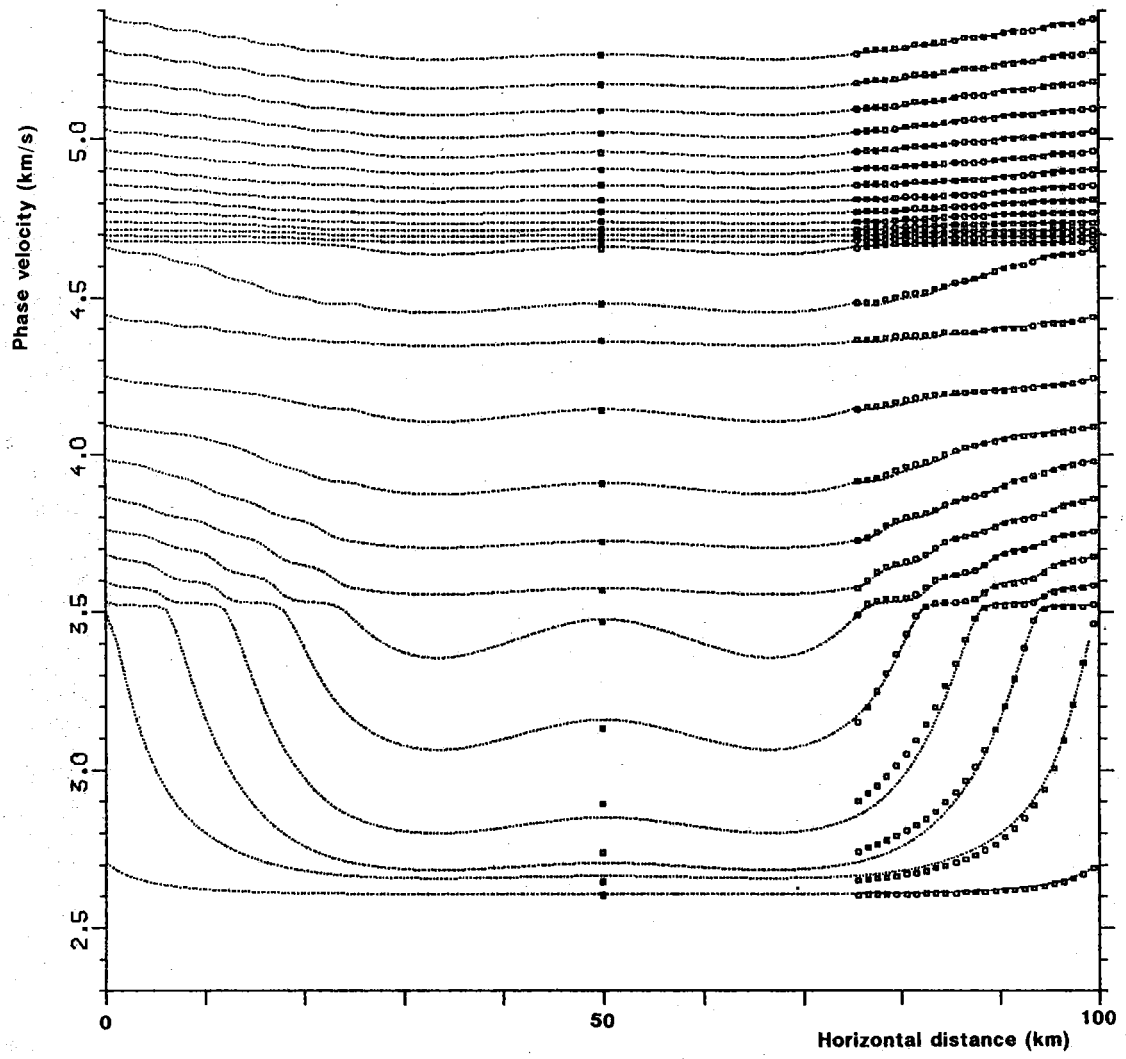

Fig. VII.4.4 Figure caption as for Fig. VII.4.3, for Love wave modes.

		Rg	Lg											Sn			P and Sv											
		0	1	2	3	4	5	6	7	8	9	10	11	12	13	14	15	16	17	18	19	20	21	22	23	24	25
Rg	0	99	3	0	1	1	1	0	1	1	0	1	0	0	0	0	0	0	0	0	0	0	0	0	0	0	0
	1	3	45	7	40	42	47	20	9	13	5	7	6	11	11	15	11	2	9	11	3	4	10	10	13	5	9
	2	0	7	17	8	7	12	56	43	4	28	22	21	20	15	17	15	5	9	19	10	4	6	5	12	14	13
	3	1	40	8	56	20	28	17	29	23	17	21	3	11	11	13	12	4	9	15	7	1	3	6	11	8	6
	4	1	42	7	20	40	29	14	36	35	17	32	22	8	15	1	6	4	3	7	2	3	4	3	8	2	3
	5	1	47	12	28	29	27	34	26	11	29	21	10	4	25	20	7	8	10	6	3	1	9	4	6	10	5
Lg	6	0	20	56	17	14	34	14	24	32	13	13	12	6	33	19	14	6	13	7	2	2	6	5	5	12	2
	7	1	9	43	29	36	26	24	50	16	3	5	18	3	12	22	3	6	8	9	3	2	5	10	6	10	3
	8	1	13	4	23	35	11	32	16	47	35	24	14	2	14	30	10	5	1	8	8	1	6	14	13	17	6
	9	0	5	28	17	17	29	13	3	35	48	16	34	12	33	10	12	7	9	4	7	5	3	13	16	8	10
	10	1	7	22	21	32	21	13	5	24	16	45	16	34	16	22	5	27	16	20	8	11	11	3	8	6	9
	11	0	6	21	3	22	10	12	18	14	34	16	59	22	21	8	16	20	19	6	7	15	5	12	19	12	7
	12	0	11	20	11	8	5	6	3	2	12	34	22	37	22	9	13	28	28	32	24	12	28	10	23	11	9
Sn	13	0	11	15	11	15	25	32	12	13	33	16	21	22	4	35	29	21	12	27	9	15	12	21	9	18	2
	14	0	15	17	13	1	20	19	22	30	10	23	8	9	35	19	15	11	13	28	15	10	14	29	27	29	10
	15	0	11	15	13	6	7	14	3	10	12	5	16	14	28	14	63	25	26	5	13	24	16	9	14	19	10
	16	0	2	5	4	4	8	7	6	6	7	27	20	28	21	10	24	66	21	15	23	21	7	0	9	11	2
	17	0	9	9	9	3	10	13	8	1	9	16	19	28	12	13	26	20	52	28	35	26	8	9	20	14	3
P	18	0	11	19	15	7	6	7	9	8	4	20	6	32	27	29	4	15	28	36	21	6	25	21	29	26	13
	19	0	3	10	7	2	3	2	3	8	7	8	7	24	10	15	13	23	35	21	69	9	7	18	17	17	14
and	20	0	4	4	1	3	1	2	2	1	5	11	15	12	15	10	25	21	26	6	9	76	16	20	17	11	8
	21	0	10	5	3	4	9	6	5	6	3	11	5	28	11	14	16	7	9	25	7	16	81	5	8	11	4
Sv	22	0	10	5	6	3	4	5	10	14	13	3	12	10	21	29	9	0	9	21	18	20	5	59	43	24	14
	23	0	13	12	11	8	6	5	6	13	16	8	19	23	9	27	15	9	20	29	17	17	8	43	26	19	41
	24	0	5	14	8	2	10	12	10	17	8	6	12	11	18	29	19	11	14	26	17	11	11	24	19	62	21
	25	0	9	13	6	3	5	2	3	6	10	9	7	9	2	10	10	2	3	13	14	8	4	14	42	21	78

Fig. VII.4.5 Transmission matrix in % for the 26 first Rayleigh wave modes at 1 Hz, after crossing the North Sea Graben perpendicularly. The matrix elements are the absolute values of amplitude transmission coefficients which carry a unit energy flux.

		Lg												Sn		Sh											
		0	1	2	3	4	5	6	7	8	9	10	11	12	13	14	15	16	17	18	19	20	21	22	23	24	25
	0	78	9	41	31	12	15	5	6	3	2	9	6	9	5	0	3	5	4	1	6	7	6	5	3	1	3
	1	9	46	23	38	28	54	7	14	12	7	23	6	8	5	1	1	4	3	5	12	14	12	8	2	5	9
	2	41	23	43	15	21	11	28	5	3	20	21	22	31	17	0	9	15	11	3	12	14	14	16	12	5	4
	3	31	38	15	43	30	26	18	9	30	16	4	1	17	7	1	4	8	7	3	15	19	18	18	11	8	7
	4	12	28	21	30	13	41	17	29	32	27	40	19	12	3	4	2	1	4	4	4	9	11	10	4	2	5
	5	15	54	11	26	41	13	19	14	21	22	15	9	16	6	4	2	2	5	3	11	19	21	18	10	12	14
Lg	6	5	7	28	18	17	19	57	40	21	10	23	27	10	4	1	2	7	6	3	14	17	13	10	7	6	9
	7	6	14	5	9	29	14	40	47	28	43	4	1	7	4	9	10	8	3	5	9	14	16	12	8	14	21
	8	3	12	3	30	32	21	21	28	43	27	39	8	9	9	6	6	7	6	6	5	9	12	10	10	16	25
	9	2	7	20	16	28	23	10	43	27	14	8	31	16	13	12	11	15	18	11	3	1	5	9	14	26	36
	10	9	23	21	4	40	14	23	4	39	8	21	20	20	20	15	13	13	20	24	14	2	10	14	12	12	24
	11	6	6	22	1	19	9	27	1	7	31	20	50	10	16	14	12	9	10	15	31	25	1	22	25	11	9
Sn	12	9	8	31	17	12	16	10	7	9	17	20	10	39	23	16	17	26	30	24	18	16	17	18	17	17	13
	13	5	4	17	7	3	5	4	5	9	13	20	16	24	84	10	6	9	11	5	3	7	5	5	11	12	9
	14	0	1	0	1	4	4	1	9	6	12	14	14	16	12	90	10	10	9	3	3	5	2	3	9	10	6
	15	3	1	9	4	2	2	2	9	6	11	12	12	17	6	11	90	12	10	4	6	6	2	3	9	9	5
	16	5	4	15	8	1	2	7	8	7	15	13	9	26	9	10	13	84	16	12	9	7	2	4	8	6	4
	17	4	3	11	7	4	5	6	3	6	18	20	10	29	11	9	10	16	80	19	11	4	3	7	9	6	4
	18	1	5	3	3	4	3	3	5	6	11	24	15	24	5	3	4	12	19	83	15	9	2	6	10	11	9
Sh	19	6	12	12	15	4	11	14	9	5	3	14	31	18	3	3	6	9	11	16	74	24	14	4	5	12	13
	20	7	14	14	19	9	19	17	14	9	1	2	25	15	7	5	6	7	4	9	24	70	26	19	7	7	12
	21	6	12	14	19	11	21	13	16	12	5	10	1	17	5	2	2	2	3	3	14	27	66	35	25	11	2
	22	5	8	16	18	10	18	10	12	10	9	14	22	18	5	3	3	4	7	6	4	19	36	53	42	26	11
	23	3	2	12	11	4	10	7	8	10	14	12	25	17	11	9	9	8	9	10	5	7	25	43	52	38	24
	24	1	5	5	8	2	12	6	14	17	26	12	11	17	12	10	9	6	6	11	12	7	11	26	38	58	37
	25	3	9	4	7	5	14	9	21	25	36	24	9	13	9	6	6	4	4	9	13	12	2	11	24	37	58

Fig. VII.4.6 Figure caption the same as for Fig. VII.4.5, for the first 26 Love wave modes.

Rayleigh modes

		Rg	Lg											Sn			P and Sv											
		0	1	2	3	4	5	6	7	8	9	10	11	12	13	14	15	16	17	18	19	20	21	22	23	24	25
Rg	0	99	2	0	0	0	1	2	0	0	0	0	0	0	0	0	0	0	0	0	0	0	0	0	0	0	0
	1	2	46	16	43	17	49	31	23	3	5	5	13	5	7	9	1	5	5	1	2	8	11	11	6	7	12
	2	0	16	26	21	46	39	6	2	39	19	10	23	12	23	13	2	13	4	4	5	9	12	7	2	13	12
	3	0	43	21	61	4	38	21	26	16	5	4	13	10	2	6	5	1	0	8	5	1	4	7	4	3	2
	4	0	17	46	4	54	31	33	19	11	16	22	8	5	13	5	3	12	3	3	5	6	11	10	2	3	9
	5	1	49	39	38	31	16	5	11	18	15	22	9	7	23	3	4	15	3	4	6	10	14	10	6	4	17
Lg	6	2	31	6	21	33	5	64	25	15	16	7	9	7	23	11	6	17	7	4	4	7	12	9	8	7	14
	7	0	23	2	26	19	11	25	42	11	41	27	26	28	11	22	8	8	7	18	6	1	6	8	10	9	7
	8	0	3	39	16	11	18	16	11	47	28	14	34	18	30	24	5	9	10	12	3	1	5	5	8	16	8
	9	0	5	19	5	16	15	16	41	28	54	23	3	4	31	19	13	15	5	5	4	6	11	7	5	14	12
	10	0	5	10	4	22	22	7	27	14	23	45	19	20	22	11	29	34	20	6	12	0	9	12	10	19	13
	11	0	13	23	13	8	9	9	26	34	3	19	46	9	17	31	14	30	24	13	14	10	3	12	20	0	8
	12	0	5	12	10	5	7	7	28	18	4	21	9	17	11	7	32	12	40	41	17	12	34	4	21	14	18
Sn	13	0	7	23	2	13	23	23	11	30	31	22	16	11	37	22	19	22	1	25	11	2	8	7	27	12	19
	14	0	9	14	6	5	3	11	22	24	18	11	32	6	21	22	14	17	11	42	3	10	29	20	23	31	17
	15	0	1	2	5	3	5	6	9	5	13	29	14	32	18	14	61	23	25	10	17	31	11	6	8	4	12
	16	0	5	13	1	12	15	17	8	9	15	33	30	12	22	17	24	54	8	8	15	21	6	17	18	13	16
	17	0	5	4	0	3	3	7	7	10	5	20	23	40	1	11	26	8	37	12	34	28	10	44	7	17	3
P	18	0	1	4	8	3	4	4	18	12	5	7	13	41	26	42	10	8	13	32	17	13	39	17	14	20	20
	19	0	2	5	5	5	6	4	6	3	4	12	14	17	11	3	17	15	34	17	66	12	24	17	24	19	19
and	20	0	8	9	1	6	11	7	1	1	6	0	10	12	2	10	31	21	28	13	11	57	31	44	3	12	5
	21	0	11	12	4	11	14	12	7	5	11	10	3	34	9	29	11	6	11	39	24	30	31	38	19	13	11
Sv	22	0	11	7	7	10	10	9	8	5	7	12	12	5	7	20	6	17	44	17	16	44	39	34	5	23	13
	23	0	6	2	4	2	6	8	10	8	5	10	20	21	27	23	8	18	7	14	24	3	19	6	38	32	54
	24	0	7	13	3	3	4	7	9	16	14	19	1	14	11	32	4	13	17	20	19	12	13	23	32	52	33
	25	0	12	12	2	9	17	14	7	8	12	13	8	18	19	17	12	16	3	20	20	5	11	13	54	33	40

Love modes

	0	1	4	3	3	3	3	2	2	1	1	0	2	0	0	0	0	0	1	0	0	1	1	3	2	1	1
	1	1	2	4	7	3	3	1	5	1	5	4	3	1	0	2	2	3	3	1	1	3	4	6	4	2	4
	2	0	1	6	3	1	1	1	2	5	2	1	5	3	3	3	1	2	3	1	1	2	2	5	2	6	3
	3	0	3	1	4	3	1	3	3	6	2	3	4	0	6	3	0	3	1	0	3	5	6	6	3	4	7
	4	0	3	8	4	2	4	1	1	2	3	1	2	1	1	0	1	2	1	1	1	1	1	1	3	2	1
	5	0	7	2	3	2	5	2	1	0	2	2	1	0	2	2	2	2	1	0	2	1	1	1	1	2	3
Lg	6	0	1	2	1	7	4	3	1	2	3	1	1	1	1	0	1	1	0	0	0	0	0	0	2	1	2
	7	0	5	2	4	2	2	1	1	1	3	3	2	0	3	0	1	1	1	1	1	0	1	1	1	2	1
	8	0	3	3	1	2	3	2	0	2	2	1	2	1	1	2	0	1	0	3	2	0	0	0	1	2	1
	9	0	3	5	2	1	3	2	2	2	4	4	0	1	0	1	2	2	0	0	1	0	0	0	1	2	2
	10	0	1	0	3	4	2	0	2	1	4	2	4	1	1	2	2	2	1	1	1	1	0	0	0	2	2
	11	0	2	5	4	0	1	1	2	1	2	1	2	3	1	1	1	1	1	1	0	1	1	0	0	3	1
	12	0	6	7	3	2	2	2	3	0	2	3	2	2	1	2	1	1	0	1	1	0	1	1	2	3	3
Sn	13	0	4	3	3	1	0	2	2	0	1	2	1	1	1	1	0	0	0	1	0	0	0	0	1	1	0
	14	0	4	5	2	2	1	2	2	0	0	1	0	1	0	2	1	0	0	1	1	0	0	0	1	1	1
	15	0	3	4	1	1	1	1	1	1	0	1	0	0	0	2	1	0	0	1	1	0	0	0	0	0	1
	16	0	1	2	1	0	1	0	1	1	1	0	0	0	0	1	1	0	0	1	0	0	0	0	0	0	1
	17	0	0	3	1	0	0	0	2	0	1	0	1	1	1	0	0	0	0	1	0	0	0	0	0	0	0
	18	0	3	3	2	1	0	2	2	1	3	0	2	1	0	1	0	0	1	0	0	0	1	0	0	0	0
Sh	19	0	3	2	3	1	2	2	1	2	3	3	0	1	0	2	0	0	1	1	0	0	2	1	1	1	0
	20	0	1	0	1	1	2	1	0	2	2	3	0	0	0	1	0	0	0	2	0	0	1	0	1	1	0
	21	0	1	1	0	1	1	1	0	1	2	1	0	0	1	1	1	0	0	1	0	0	0	0	1	1	0
	22	0	0	1	1	0	0	1	0	0	1	1	0	1	1	0	1	0	0	0	0	0	1	0	0	1	0
	23	0	0	1	1	1	1	1	0	0	1	2	1	0	0	1	0	0	0	1	0	0	1	0	1	0	0
	24	0	1	2	2	2	0	1	1	0	2	2	1	1	1	1	1	0	0	0	0	0	0	0	0	0	0
	25	0	1	1	0	2	1	1	2	1	1	3	2	1	1	0	0	0	0	1	0	0	0	0	0	1	1

Fig. VII.4.7 Figure caption the same as for Fig. VII.4.5, for propagation at an angle across the North Sea Graben, with a slowness of 1.0 s/km in the y-direction.

		Lg												Sn		Sh												
		0	1	2	3	4	5	6	7	8	9	10	11	12	13	14	15	16	17	18	19	20	21	22	23	24	25
Love modes	0	89	8	13	29	13	13	5	12	5	5	1	8	6	3	3	2	1	1	3	3	0	0	0	1	0	1
	1	8	42	31	31	13	46	33	6	8	6	1	21	23	15	15	12	5	2	10	15	4	3	1	2	4	2
	2	13	31	26	26	44	24	20	15	28	11	9	33	26	14	15	12	5	6	6	13	9	2	0	0	2	2
	3	29	31	26	68	25	10	14	2	15	7	7	8	19	11	13	10	5	4	1	2	1	1	0	2	3	1
	4	13	13	44	25	22	50	18	36	21	11	21	8	16	14	11	7	4	4	4	3	7	3	0	3	1	4
	5	13	46	24	10	50	9	25	17	10	17	12	13	27	20	19	15	6	6	15	12	4	1	1	4	7	1
Lg	6	5	33	20	14	17	25	41	15	32	45	21	22	12	10	9	9	5	1	11	12	5	6	2	5	5	8
	7	12	6	15	2	36	17	15	38	33	36	18	23	8	5	4	6	5	6	27	32	16	7	6	6	15	1
	8	5	8	28	15	21	10	32	33	51	4	18	23	13	3	7	8	5	5	20	24	15	13	8	9	17	9
	9	5	6	11	7	11	17	45	36	4	11	17	28	14	5	8	8	8	7	3	13	27	23	15	23	25	28
	10	1	1	9	7	22	12	21	19	18	17	55	10	7	11	7	7	7	8	19	12	14	8	13	28	20	41
	11	8	21	33	8	8	13	22	23	23	29	10	53	19	10	9	4	3	5	12	16	8	13	10	13	19	22
Sn	12	6	23	26	19	16	27	12	8	13	14	7	19	55	21	23	18	11	11	6	6	14	12	3	17	20	13
	13	3	15	14	11	14	20	10	5	2	5	11	10	19	68	30	24	16	7	5	4	9	7	2	7	20	26
	14	3	16	15	13	11	19	10	4	7	8	7	9	24	28	73	25	17	7	4	6	6	3	2	2	5	19
	15	2	12	12	10	8	15	9	6	8	8	7	4	19	24	23	77	21	12	6	6	4	0	0	2	4	21
	16	1	5	5	5	4	7	5	5	5	8	7	3	11	16	16	20	86	18	10	6	2	4	4	2	5	19
	17	1	2	6	4	4	6	1	6	5	7	8	5	11	7	7	12	18	90	14	8	2	9	9	1	8	12
	18	3	10	6	1	4	15	11	27	21	3	20	12	7	5	4	6	10	14	79	20	4	9	10	0	12	6
Sh	19	3	15	13	2	3	12	12	32	24	13	12	16	6	4	6	6	6	8	20	70	23	15	6	7	11	9
	20	0	4	9	1	7	4	5	16	15	27	14	8	14	9	6	4	2	2	4	23	58	43	30	23	19	6
	21	0	3	2	1	4	1	6	7	13	23	8	13	12	8	3	0	4	9	9	15	43	46	49	31	22	12
	22	0	1	0	0	0	1	2	6	8	15	12	10	3	2	2	0	4	9	10	6	30	49	62	37	14	10
	23	1	2	0	2	3	4	5	6	9	23	28	13	17	7	2	2	2	1	0	7	23	31	37	49	47	11
	24	0	4	2	3	1	7	5	15	17	25	20	19	20	20	5	4	5	8	12	11	19	22	14	46	37	43
	25	1	2	2	1	4	1	8	1	9	29	41	22	13	26	19	21	19	12	6	9	6	12	10	11	43	44
Rg	0	1	1	0	0	0	0	0	0	0	0	0	0	0	0	0	0	0	0	0	0	0	0	0	0	0	0
Rayleigh modes	1	4	2	1	3	3	7	1	4	3	3	1	3	6	4	4	3	1	0	3	3	1	1	0	0	1	1
	2	3	4	6	1	8	2	2	1	3	5	0	5	7	3	5	4	2	3	3	2	0	1	1	1	2	1
	3	3	7	3	4	4	3	1	4	1	2	3	4	3	3	2	1	1	1	2	3	2	0	1	1	2	0
	4	3	3	1	3	2	2	7	2	2	1	4	0	2	1	2	1	0	0	1	1	1	1	0	1	2	2
	5	3	3	1	1	4	5	4	2	3	3	2	1	2	0	1	1	1	0	0	2	2	1	0	1	0	1
Lg	6	2	1	1	3	1	2	3	1	2	2	0	1	2	2	1	1	0	0	2	2	1	1	1	1	1	1
	7	2	5	2	3	1	1	1	1	0	2	2	2	3	2	1	1	1	2	2	1	0	0	0	0	1	2
	8	1	1	5	6	2	0	2	1	2	2	1	1	0	0	0	1	1	0	1	2	2	1	0	0	0	1
	9	1	5	2	2	3	2	3	3	2	4	4	2	2	1	0	0	1	1	3	3	2	2	1	1	2	1
	10	0	4	1	3	1	2	1	3	1	4	2	1	3	2	1	1	0	0	0	3	3	1	1	2	2	3
	11	2	3	5	4	2	1	1	2	2	0	4	2	2	1	0	0	0	1	2	0	0	0	0	1	1	2
Sn	12	0	1	3	0	1	0	1	0	1	1	1	3	2	1	1	0	0	1	1	1	0	0	1	0	1	1
	13	0	0	3	5	1	2	1	3	1	0	1	1	1	1	0	0	0	1	0	0	0	1	1	0	1	1
	14	0	2	3	4	0	2	0	0	2	1	2	1	2	1	2	2	1	0	1	2	1	1	0	1	1	0
P and Sv	15	0	2	1	0	1	2	1	1	0	2	2	1	1	0	1	1	1	0	0	0	0	1	1	0	1	0
	16	0	3	2	3	2	2	1	1	1	2	2	1	1	0	0	0	0	0	0	0	0	0	0	0	0	0
	17	1	3	3	1	1	1	0	1	0	0	1	1	0	0	0	0	0	0	1	1	0	0	0	0	0	0
	18	0	1	1	0	1	0	0	1	3	0	1	1	1	1	1	1	1	1	0	1	2	1	0	1	0	1
	19	0	1	1	3	1	2	0	1	2	1	1	0	1	0	1	1	0	0	0	0	0	0	0	0	0	0
	20	1	3	2	5	1	1	0	0	0	0	1	1	0	0	0	0	0	0	0	0	0	0	0	0	0	0
	21	1	4	2	6	1	1	0	1	0	0	0	1	1	0	0	0	0	0	1	2	1	0	1	1	0	0
	22	3	6	5	6	1	1	0	1	0	0	0	0	1	0	0	0	0	0	0	1	0	0	0	0	0	0
	23	2	4	2	3	3	1	2	1	1	1	0	0	2	1	1	0	0	0	0	1	1	1	0	1	0	0
	24	1	2	6	4	2	2	1	2	2	2	2	3	3	1	1	0	0	0	0	1	1	1	1	0	0	1
	25	1	4	3	7	1	3	2	1	1	2	2	1	3	1	1	1	1	0	0	0	0	0	0	0	0	1

Fig. VII.4.8 Figure caption the same as for Fig. VII.4.6, for propagation at an angle across the North Sea Graben, with a slowness of 1.0 s/km in the y-direction.

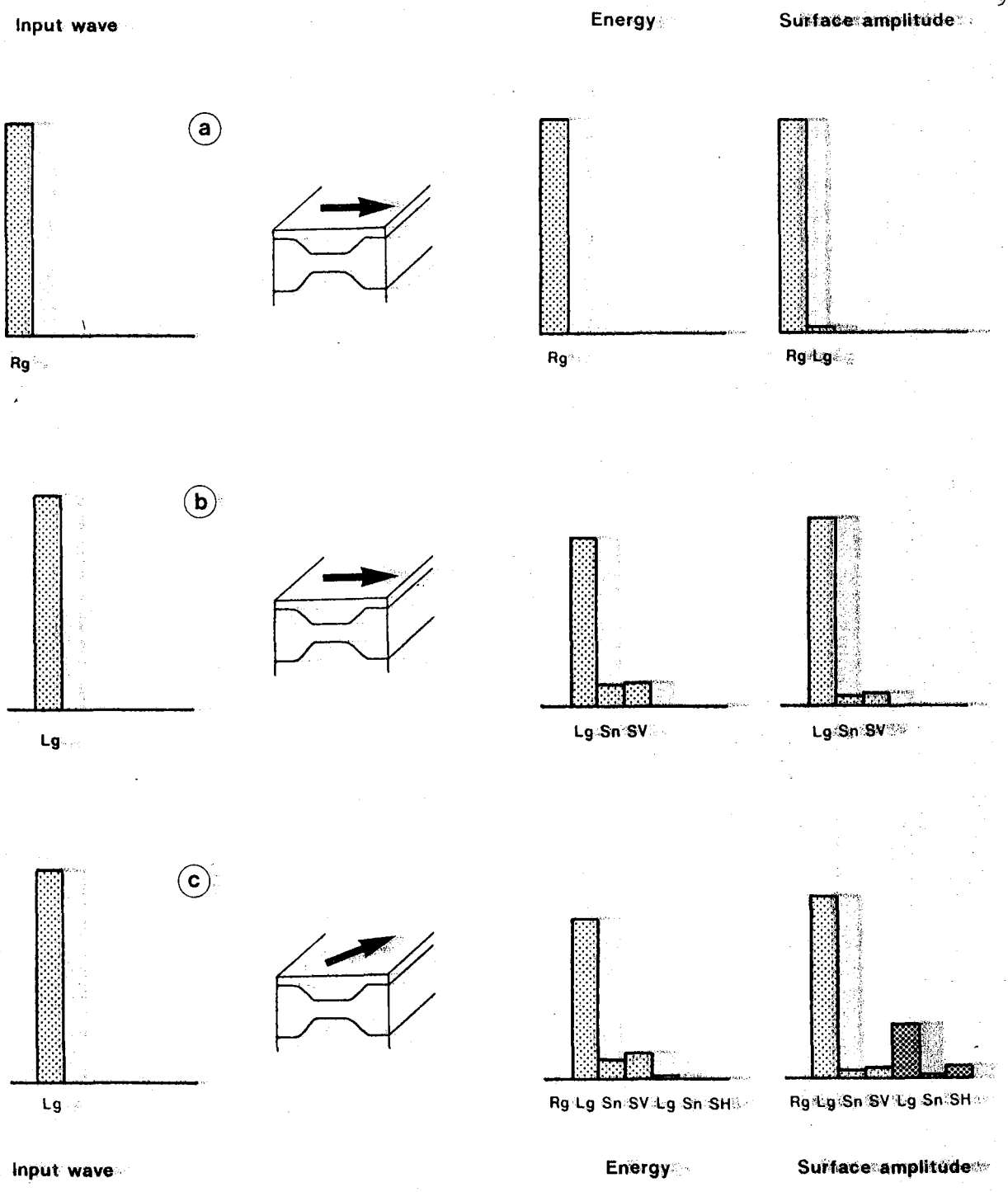

Fig. VII.4.9 Wavetrain transmission across the North Sea Graben at 1 Hz for incoming Rg and Rayleigh-type Lg wavetrains. The repartition of the total energy and the surface amplitude of the wavetrains at the output of the model are plotted normalized to the energy or amplitude of the input wave. Small-dotted pattern indicates Rayleigh-type wavetrain and large-dotted pattern indicates Love-type wavetrain. The arrow indicates the propagation direction in the model.

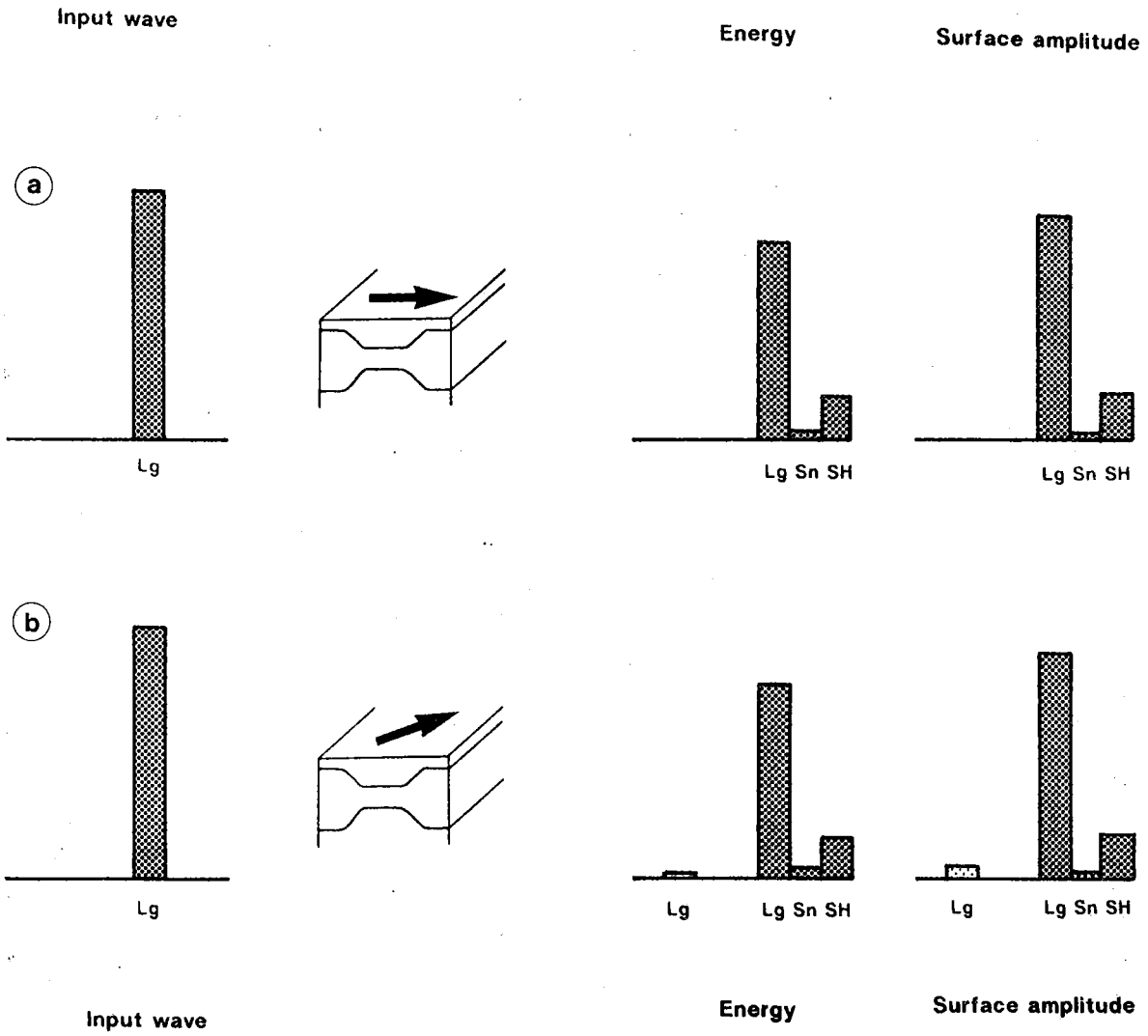

Fig. VII.4.10 The same as for Fig. VII.4.9, for incoming Love-type Lg wavetrains.

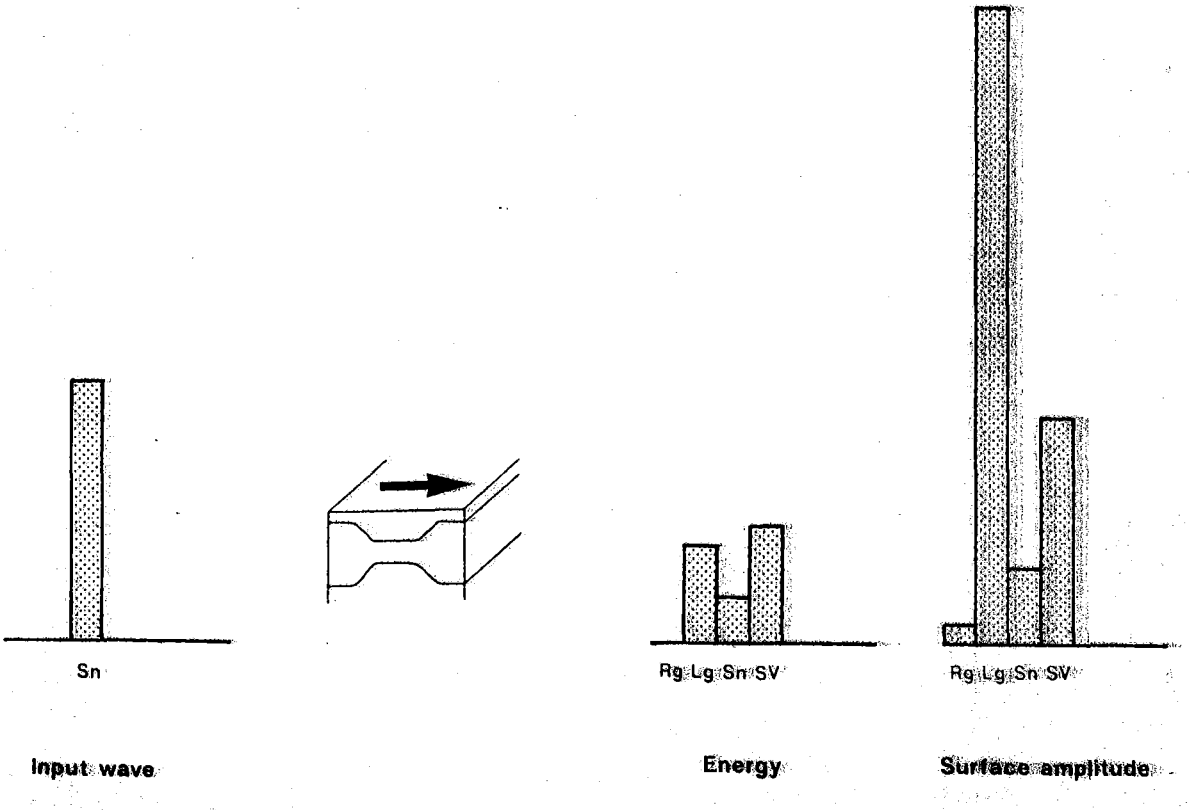

Fig. VII.4.11 The same as for Fig. VII.4.9, for an incoming Sn wave.